Desalination for the Environment
Clean Water and Energy
May 11-15, 2014, Limassol, Cyprus

UNIVERSITÀ DEGLI STUDI DI PALERMO

Scuola Politecnica
Dipartimento di Ingegneria Chimica, Gestionale, Informatica e Meccanica (DICGIM), viale delle Scienze (Ed.6), 90128 Palermo, Italy

CFD modelling of profiled membranes channels for Reverse Electrodialysis

Gurreri L., Ciofalo M., Cipollina A., Tamburini A., Van Baak W., Micale G.

***e-mail address: luigi.gurreri*@unipa.it**

RED CHANNELS

Channel geometry → Fluid Dynamics → Performance

- Hydraulic friction
- Concentration Polarization

Separation of membranes

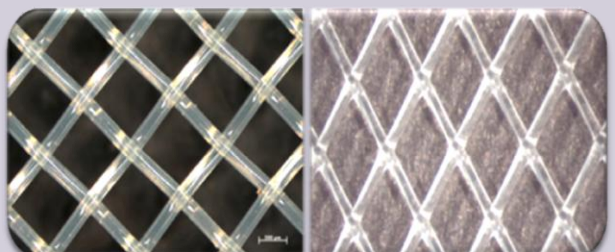

Spacers

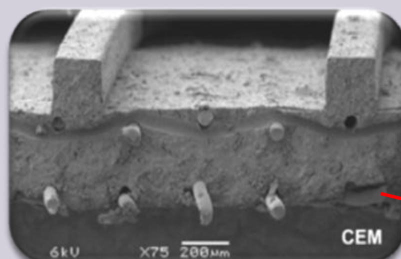

Profiled Membranes (PM)

Advantages

- Lower ohmic resistance
- Lower friction factor
- Shadow effect avoided
- Lower costs

OBJECTIVES, TOOLS AND ACTIVITIES

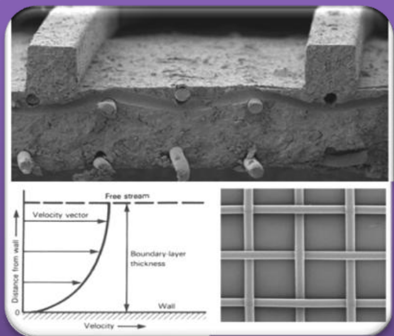

Objective: prediction of fluid flow and mass transfer in channels with PM for RED stacks

- Comparison with empty and spacer-filled channels
- Process efficiency

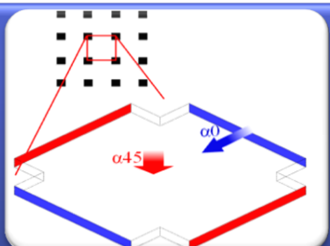

Tools: 3D-Computational Fluid Dynamics (CFD) modelling

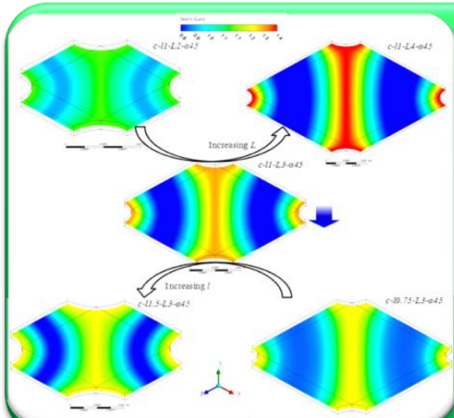

Activities: parametric analysis

- Channel geometry: shape, size and pitch of profiles
- Channel orientation (fluid flow direction)
- Reynolds numbers typical of RED applications

NUMERICAL METHODOLOGIES

CASES INVESTIGATED

Profiles in *square pitch*

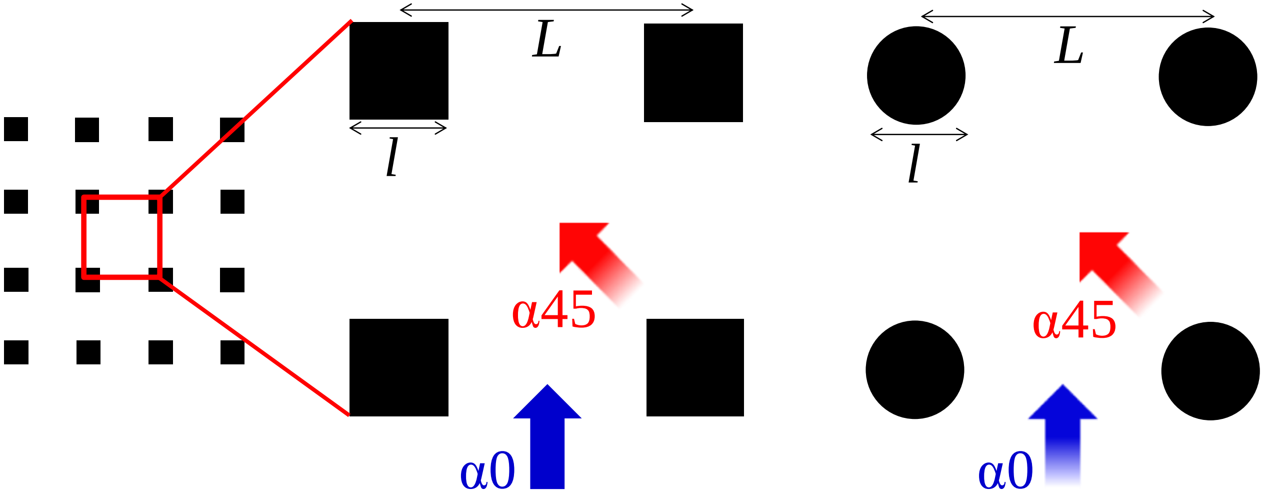

Profiles' s shape

- Square (s)
- Circular (c)

Fluid flow direction α

1) 0°
2) 45°

Sizes

h = 160 µm

l = 0.75, 1, 1.5 mm

L = 2, 3, 4 mm

(indicated as *l0.75, l1, l1.5* and *L2, L3, L4)*

Reynolds number *Re*

0.5, 2, 8, 32

Empty ch. and **spacer-filled ch.** for comparison

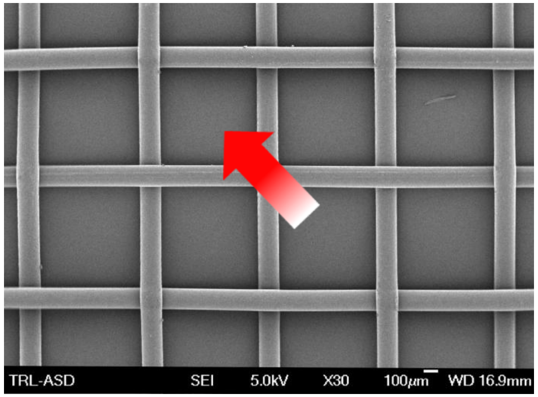

Woven spacer

h = 0.16 mm

mesh length = 0.46 mm

GOOD MIXING

CFD MODELING

The finite volumes code **Ansys-CFX 14** was employed to discretize and solve the governing equations (Newtonian and incompressible fluid). **Steady** regime at all flow rates investigated

$$\vec{\nabla} \cdot \vec{u} = 0$$

$$\rho \frac{\partial \vec{u}}{\partial t} + \rho \vec{u} \vec{\nabla} \cdot \vec{u} = -\vec{\nabla} p + \mu \nabla^2 \vec{u} + \vec{P}$$

Body force → fluid motion in a periodic domain

$$\vec{\nabla}\left(\tilde{C}\vec{u}\right) = \vec{\nabla}\left[D \frac{b}{b + \left(a - M_e\right)\left(\tilde{C} + ks\right)} \vec{\nabla}\tilde{C} \right] - ku_s$$

NaCl solution at T = 25 °C	Molarity [mol/l]	Density [kg/m³]	Viscosity [Pa s]	Diffusivity [m²/s]
Seawater	0.5	1017.2	9.31e-04	1.47e-09

BASIC EQUATIONS*

Transport equation for a binary electrolyte

Multicomponent diffusion equation (Stefan-Maxwell)

$$C_i \overline{\nabla} \mu_i = \sum_j K_{ij}\left(\overline{u}_j - \overline{u}_i\right) = RT \sum_j \frac{C_i C_j}{C_T D_{ij}}\left(\overline{u}_j - \overline{u}_i\right)$$

Electroneutrality condition binary electrolyte

$$z_+ C_+ = -z_- C_-$$

solvent velocity ≈ *u*

salt diffusivity

solvent concentration

transport number

$$\underbrace{\frac{\partial C}{\partial t}}_{\text{Accumulation}} + \underbrace{\overline{\nabla}\left(C\overline{u}_0\right)}_{\text{Convection}} = \underbrace{\overline{\nabla} \cdot \left[D \left(1 - \frac{d \ln C_0}{d \ln C} \right) \overline{\nabla} C \right]}_{\text{Diffusion}} - \underbrace{\frac{\overline{i} \cdot \overline{\nabla} t_i^0}{z_i \nu_i F}}_{\text{Migration}}$$

Accumulation Convection Diffusion Migration

J.S. Newman, Electrochemical Systems, Second Edition, 2nd edition, Prentice Hall, Englewood Cliffs, NJ (1991)

K. Kontturi, L Murtomäki, J.A. Manzanares, Ionic Transport Processes In Electrochemistry and Membrane Science, Oxford University Press (2008)

CFD MODELLING DEVELOPMENT

Implementation of transport equations

Assuming density as a linear function of *C*

$$\rho = aC + b$$

Diffusive term

$$\left(1 - \frac{d\ln C_0}{d\ln C}\right) = \frac{\rho - C\dfrac{d\rho}{dC}}{C_0 M_0} = \frac{b}{b + \left(a - M_C\right)C}$$

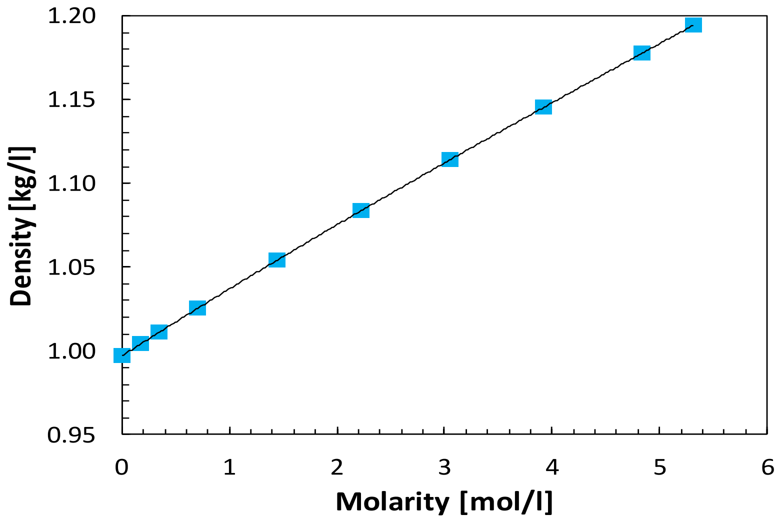

CFD MODELLING DEVELOPMENT

Implementation of transport equations

Migrative term

$$\frac{\partial C}{\partial t}+\overline{\nabla}\left(C\overline{u}_0\right)=\overline{\nabla}\cdot\left[D\frac{b}{b+\left(a-M_C\right)C}\overline{\nabla}C\right]-\frac{\overline{i}\cdot\overline{\nabla}t_i^0}{z_i\nu_iF}$$

- Current density
- Equations system not closed
- Above transport equation can be solved when
  - coupled with other equations → entire stack as domain
  - or when current density distribution is known (spacer-less channel)

CFD MODELLING DEVELOPMENT

Implementation of transport equations

Simulations of an empty channel

- Concentration profiles were unaffected by the migrative term
- Migrative term is negligible compared to the diffusive one
- → Migrative flux is quite uniform

most unfavourable case (low concentration and high current density)

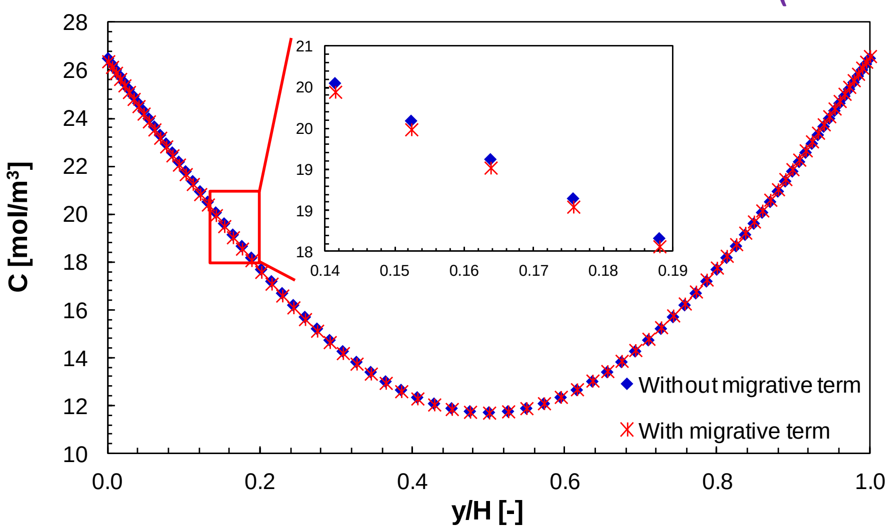

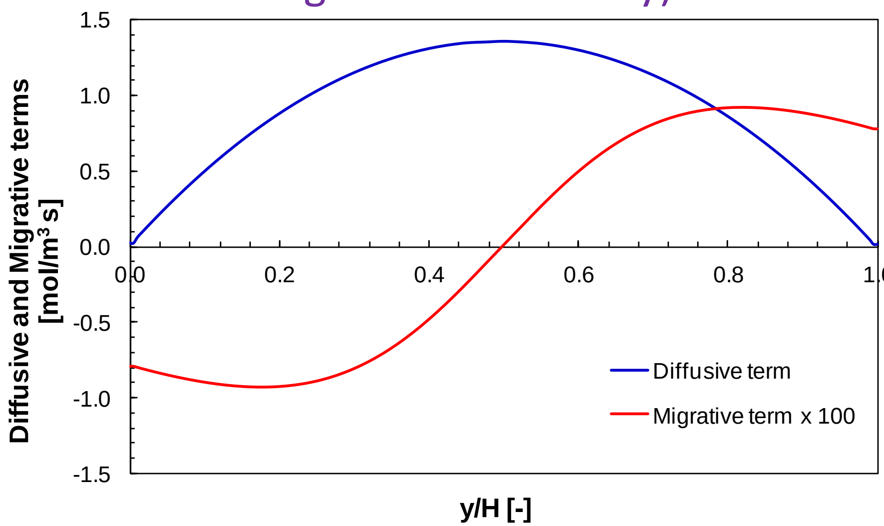

$$\frac{\partial C}{\partial t}+\bar{\nabla}\left(C\bar{u}_0\right)=\bar{\nabla}\cdot\left[D\frac{b}{b+\left(a-M_C\right)C}\bar{\nabla}C\right]-\cancel{\frac{\bar{i}\cdot\bar{\nabla}t_i^0}{z_i\nu_i F}}$$

Migrative term neglected

MODELLING APPROACH

Transport equation implemented for Unit Cell

Fully developed flow → Linear variation of concentration along the flow direction (s)
Periodic boundary conditions despite the change of the bulk concentration

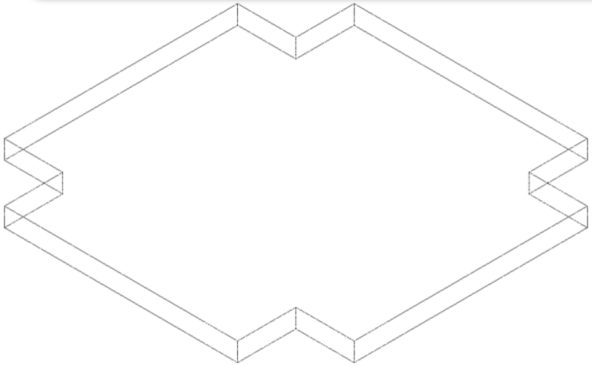

$$C = \tilde{C}(x, y, z, t) + k \cdot s$$

Conc. gradient

Periodic concentration

Fluid flow direction

Transport equation for the electrolyte in unit cell

$$\frac{\partial \tilde{C}}{\partial t} + \vec{\nabla}\left(\tilde{C}\vec{u}\right) = \vec{\nabla}\left[D \frac{b}{b + \left(a - M_e\right)\left(\tilde{C} + ks\right)} \vec{\nabla}\tilde{C}\right] - ku_s$$

$$k = \frac{Q_{TOT}}{V \cdot u_{s,ave}}$$

$$Q_{TOT} = J \cdot (A_{CEM} + A_{AEM})$$

Ingoing flux throug membrane

MODELLING APPROACH

Computational domain

One channel

No double layer

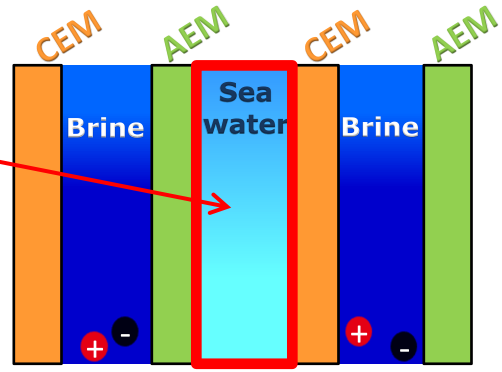

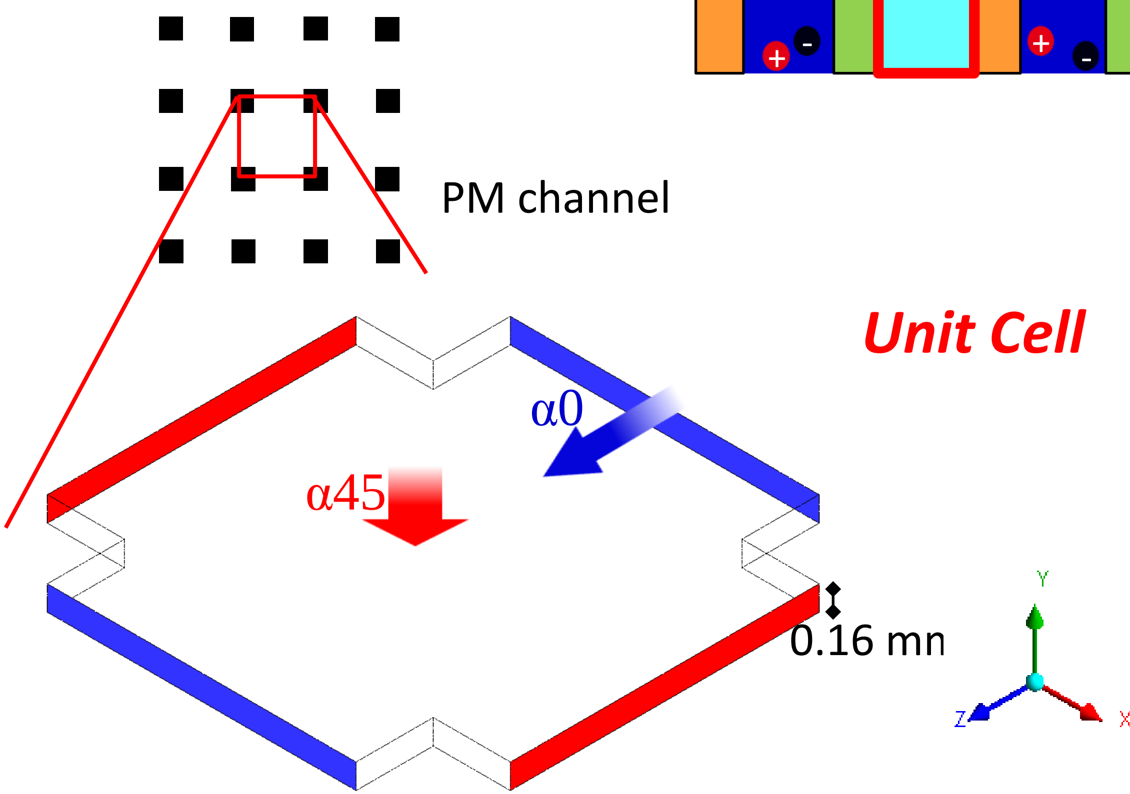

Spacer-filled channel

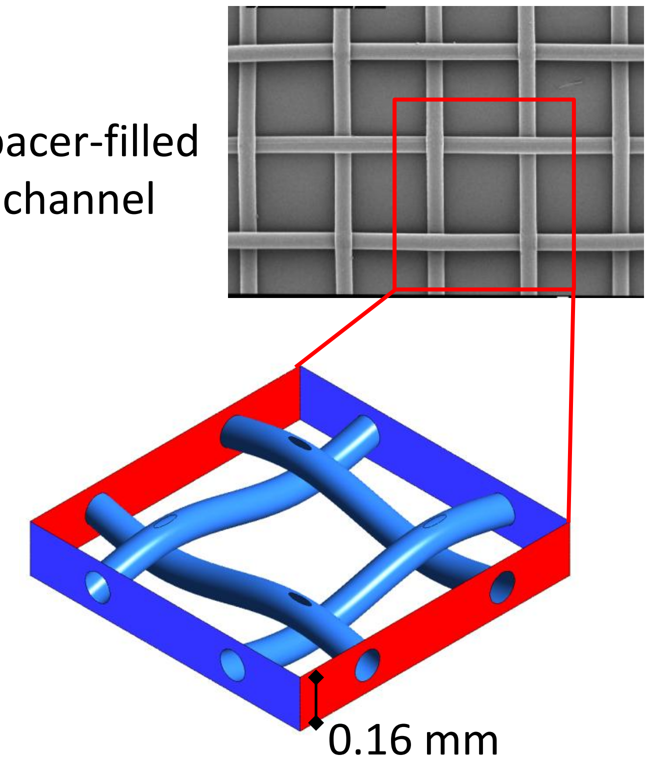

MODELLING APPROACH

Wall boundary at membrane-solution interface

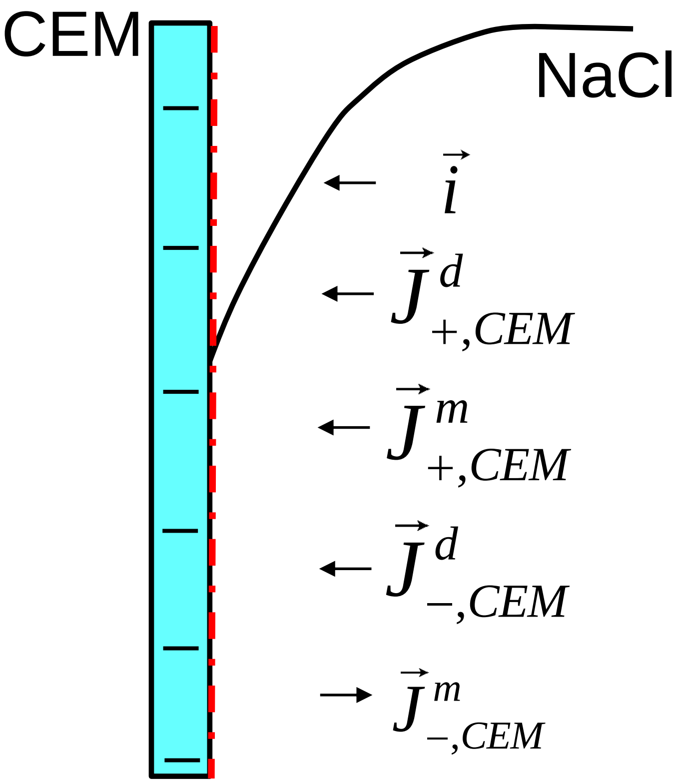

$$\vec{J}_i^m = \frac{t_i^0}{z_i F}\vec{i}$$

$$\alpha = 1 \quad \Rightarrow \quad \vec{J}^{tot}_{-,CEM} = 0 = \vec{J}^{d}_{-,CEM} + \vec{J}^{m}_{-,CEM}$$

$$\vec{J}^{d}_{-,CEM} = -\vec{J}^{m}_{-,CEM} = -\frac{t_-^0}{z_- F}\vec{i}$$

$$\vec{J}^{d}_{CEM} = \frac{\vec{J}^{d}_{-,CEM}}{\nu_-} = -\frac{t_-^0}{\nu_- z_- F}\vec{i} \approx \frac{0.5}{F}\vec{i}$$

Uniform flux at the **membrane-solution interfaces**, corresponding to *i* = 200 A/m^2, a provisional value achievable in systems optimized for high power density by the use of highly conductive solutions and membranes

MODELLING APPROACH

Wall boundary at the lateral surfaces

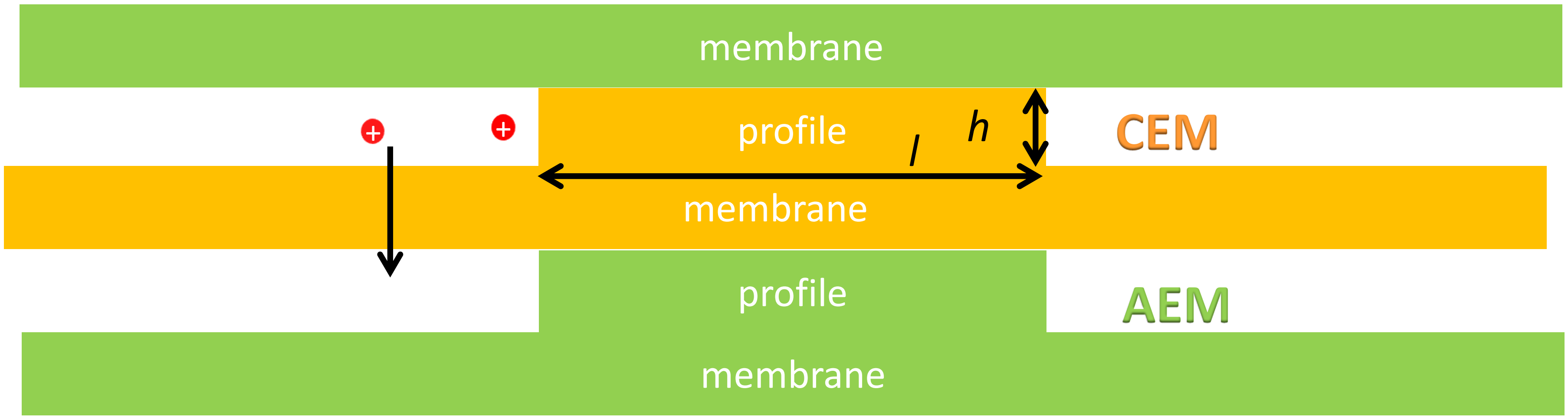

Flux set **nil** at the **lateral walls** (fluid-membrane profile interfaces)

• Highly conductive solutions as seawater and profiles with high length (*l*) compared to the height (*h*) → ion close to the membrane profile would across easier solution and membrane rather than profile and membrane

•Areal resistance per unit of thickness ≈ 3 Ωm for membr., ≈ 0.2 Ωm for seawater

• Ionic current across the membranes' profiles expected low due to their small area, → its contribution to the overall current is negligible

MODELLING APPROACH

Mesh and *grid dependence analysis*

Hexahedral mesh: 30 volumes in the vertical direction (ch. thickness)

Grid dependence: 10 to 60 vertical divisions
- results independent of the discretization degree
- computational savings

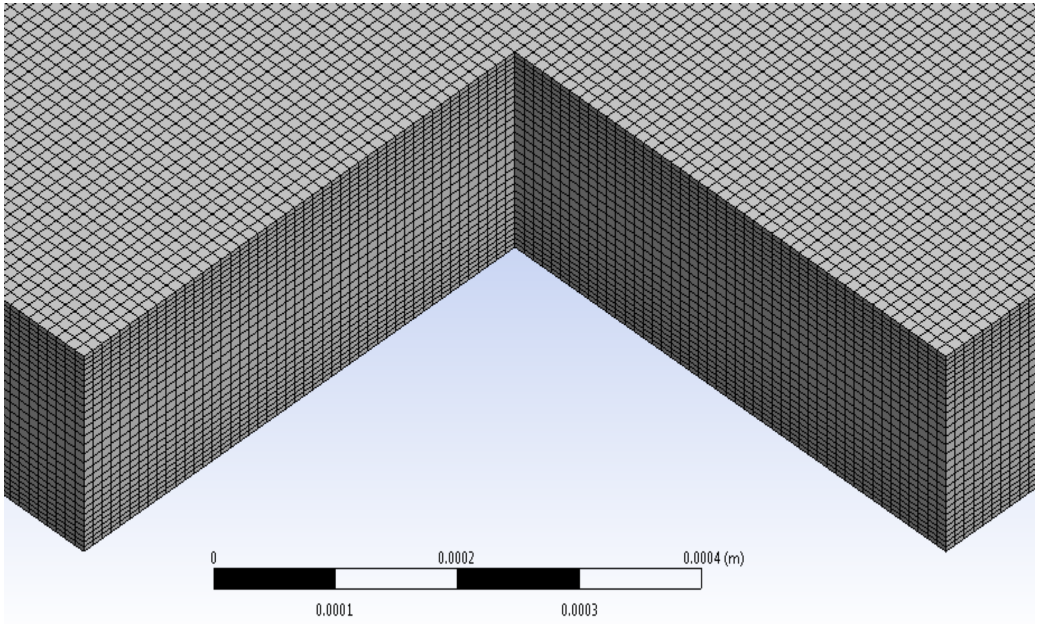

➢~ $1{\cdot}10^6$ to ~$4{\cdot}10^6$ volumes

Spacer-filled channel: hybrid mesh with tetrahedra near the filaments and hexahedrons elsewhere

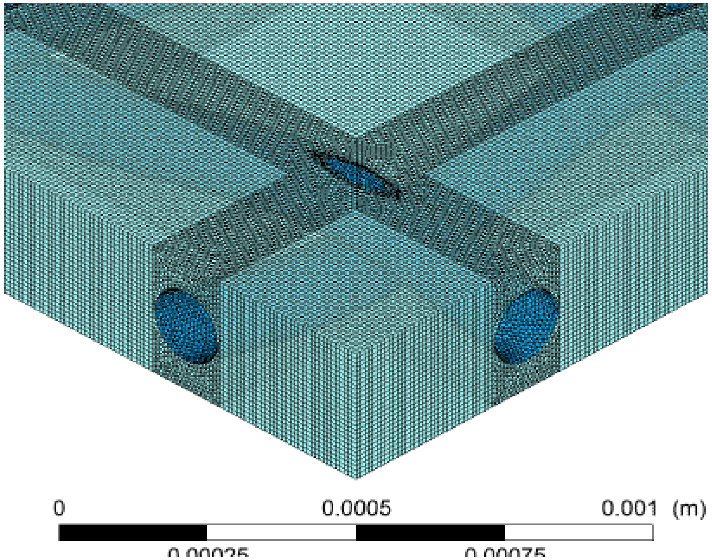

$1.6{\cdot}10^6$ volumes

RESULTS

Influence of profiles' shape, flow attack angle and Re

(*l* = 1 mm, *L* = 3 mm)

VELOCITY FIELD

Plane *x-z* middle, Re = 8

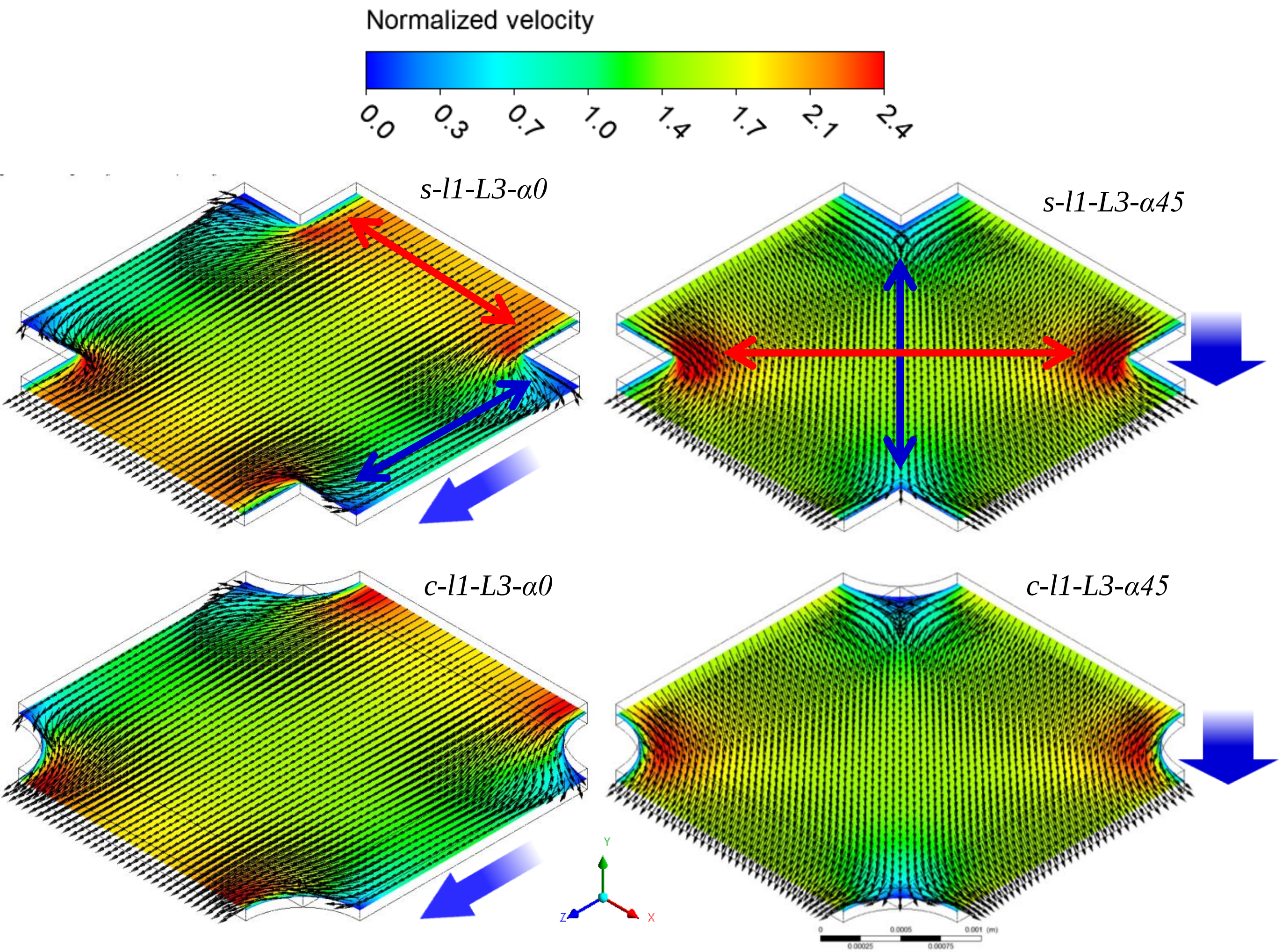

- Full thickness obstacles → absence of vertical component of velocity
- Zigzag flow path
- Symmetry features
- Velocity increases between adjacent profiles
- **Calm zones** upstream and downstream the profiles, especially for *α0*
- Less homogeneous velocity distribution for square shape

CONCENTRATION FIELD

Plane *x-z* middle, Re = 8

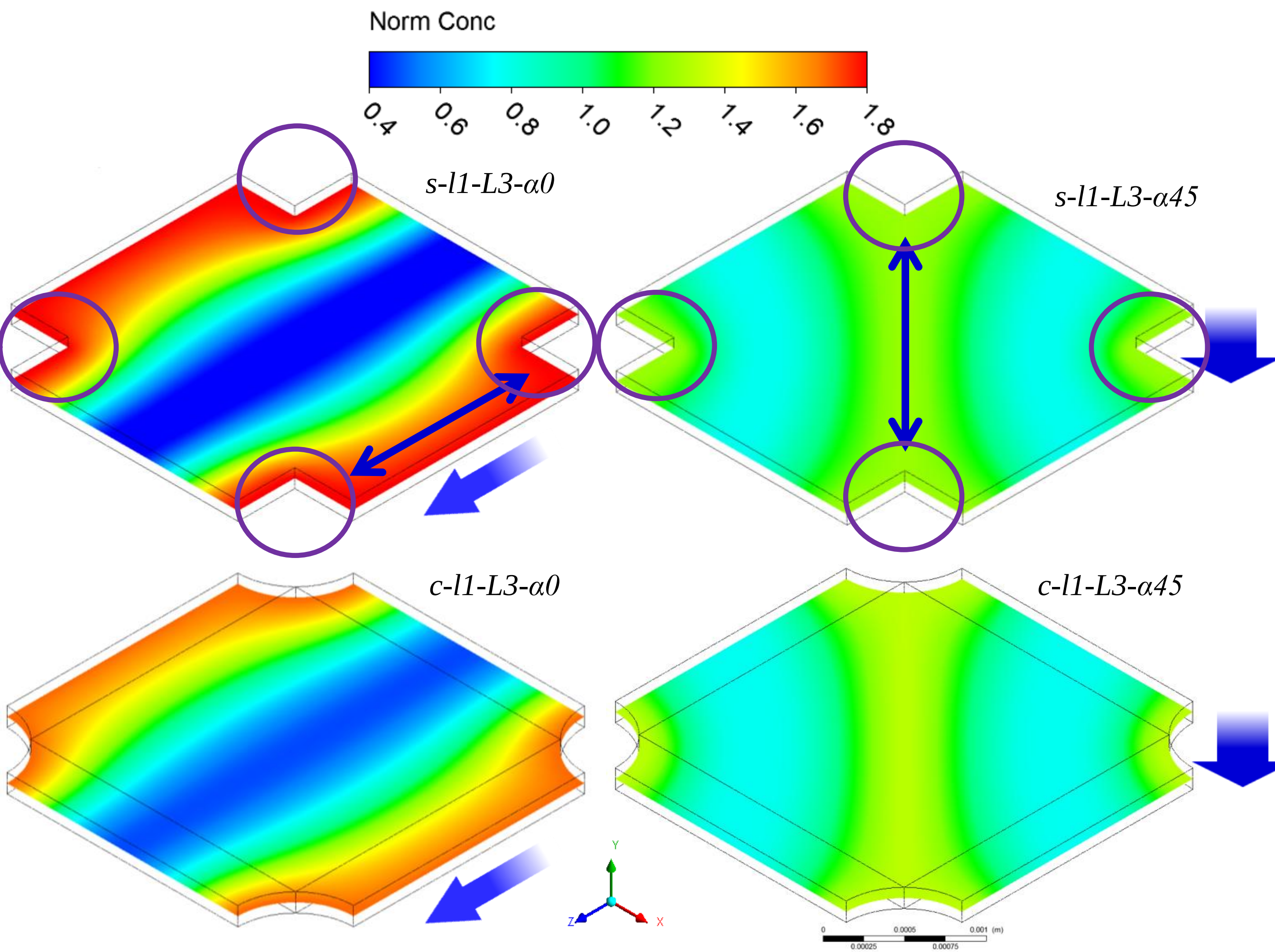

- Highest concentration (maximum polarization) in: (i) the calm regions; (ii) all around the profiles due to zero velocity at the walls
- ***α*** more **crucial** than profile shape
- *α45* → more uniform concentration field, particularly for case of the square profile (*s-l1-L3-α45*)

CONCENTRATION FIELD

Concentration profiles, c-l1-L3-α45

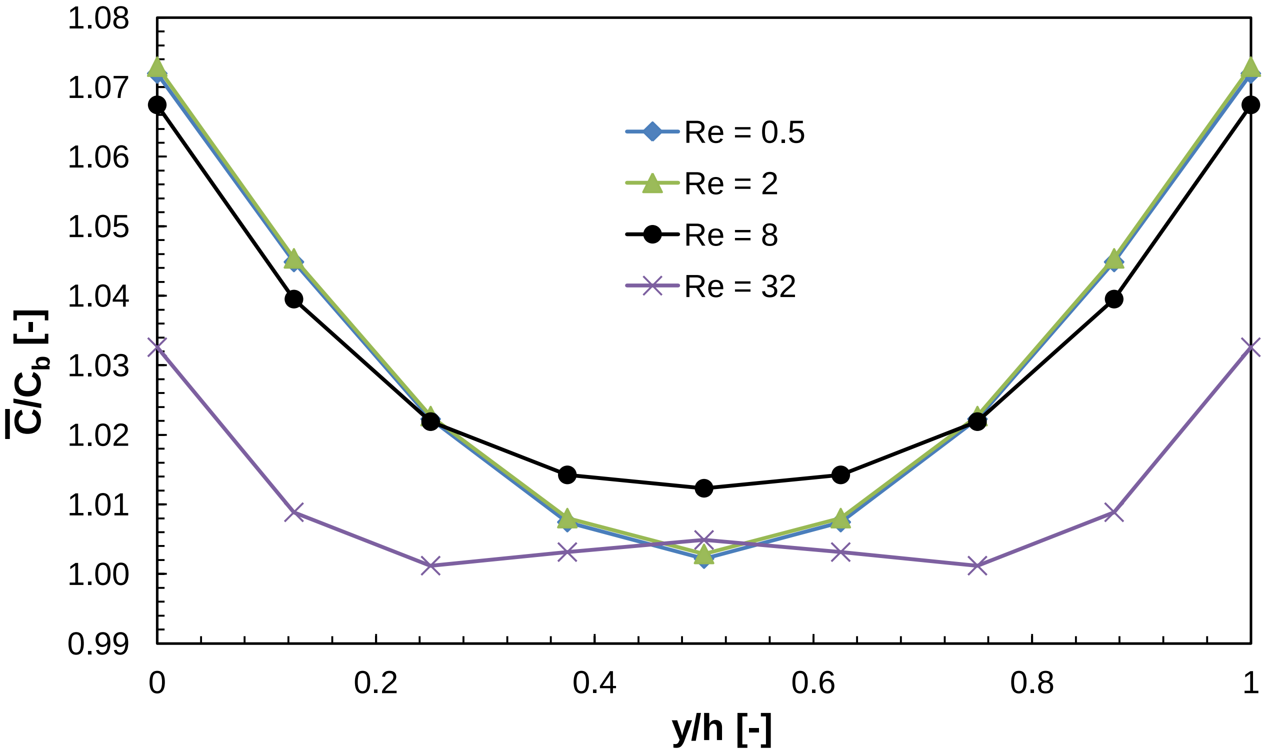

- Higher **Re** → increased inertial phenomena as separation, recirculation, and reattachment → fluid **mixing enhancement**

- Equal profiles obtained at Re = 0.5 and Re = 2, due to **creeping flow** conditions at very low Re numbers

FRICTION FACTOR

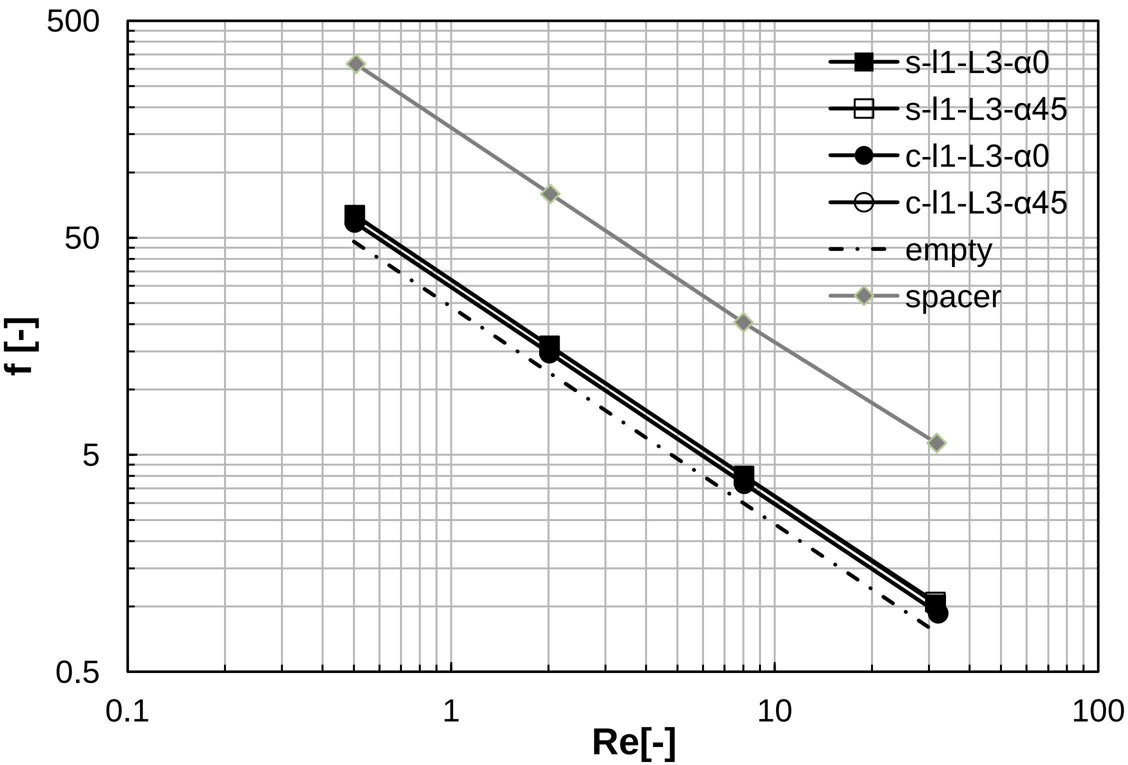

$$f = \frac{\Delta p}{l} \frac{d_h}{2 \rho u_{s,mean}^2}$$

$$f = A Re^n$$

- The presence of obstacles causes ***f*** **slightly higher than the empty ch**.
- Much higher pressure drop for the **spacer-filled ch**.
- ***α*** has irrelevant effects
- The square **shape** implies *f* a bit higher than the circular one
- At the lowest Re numbers, *n = -1* was found → creeping flow regime
- At higher Re, *n* deviates from -1, since the obstacles induce increasing inertial effects → flow fields not self-similar

POWER NUMBER

$$Pn = \mathrm{SPC}\frac{\rho^2 h^4}{\mu^3} = \frac{1}{8} f\, Re^3 \qquad \mathrm{SPC} = \frac{\Delta p}{l} u_{s,mean}$$

$$Pn = B Re^m$$

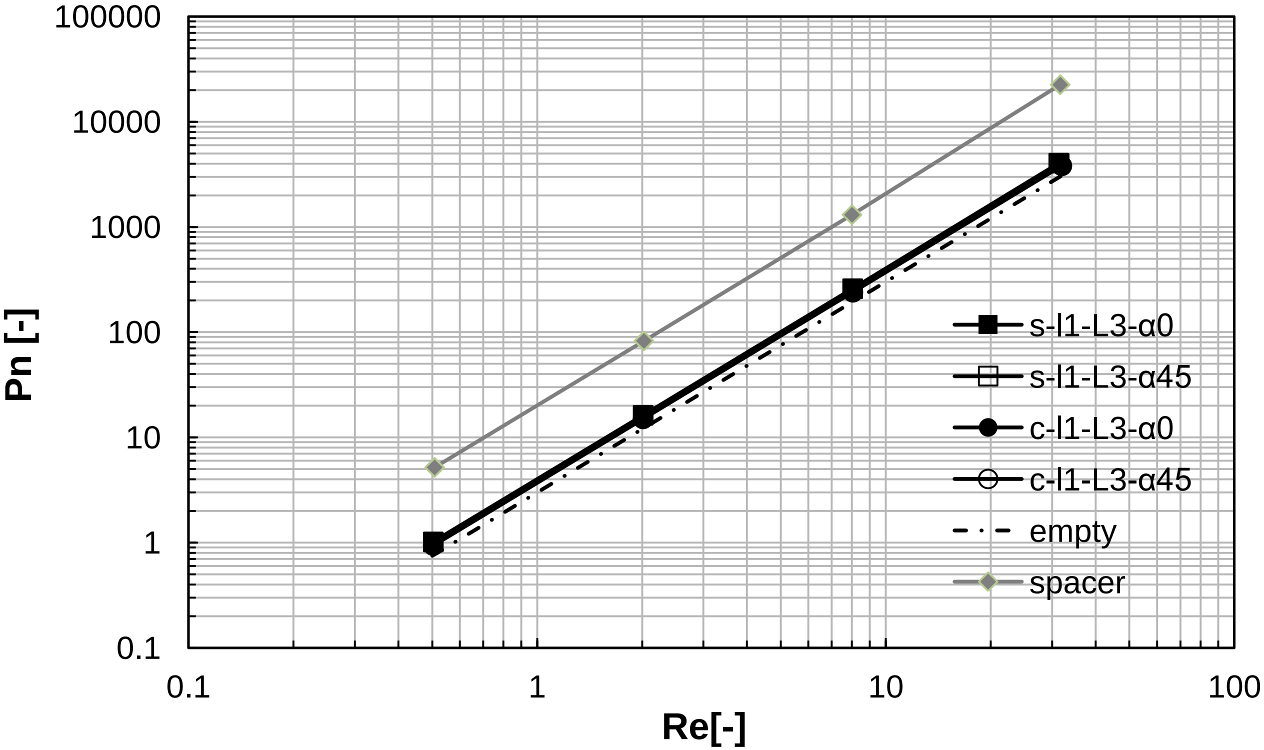

- The **square shape** requires Pn increased of about 8% with respect to the circular shape
- ***α*** is **irrelevant**
- **Circular and square profiles** provide an increment in Pn of about **23%** and **33%** respect to the **empty ch**.
- The **spacer-filled ch.** requires pumping costs increased of **~570%**

Results: Influence of profiles' shape, flow attack angle and Re (l1-L3)

POLARIZATION FACTOR

$$\theta = \frac{C_b}{C_i} < 1$$

Desired condition: **θ=1**, **flat profile**

$$E_{OCV} - \eta_{BL} = 2\alpha_m \frac{RT}{F}\left[\ln\left(\frac{\hat{C}_b^{conc}}{\hat{C}_b^{dil}}\right) + \ln\left(\theta^{conc}\theta^{dil}\right) + \ln\left(\frac{\overline{\gamma}_w^{conc}}{\overline{\gamma}_w^{dil}}\right)\right]$$

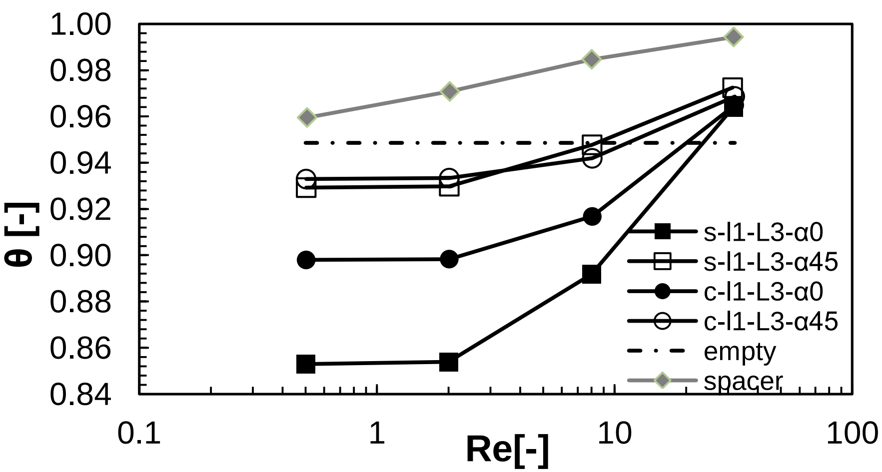

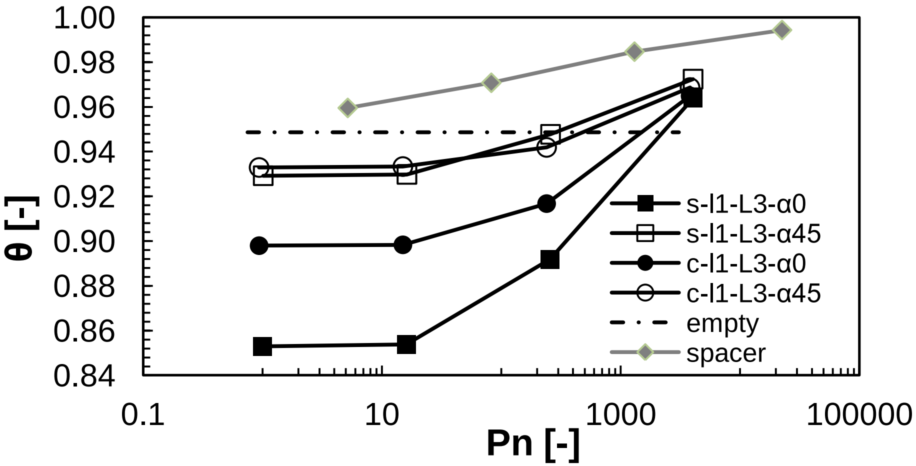

- .Very slight θ increase at the lowest Re due to a **creeping flow**
- **Mixing not favored at low Re** due to the calm regions → θ lower than the empty ch.
- **Higher Re/Pn**: **mass transfer enhancement** and all the configurations provide similar θ approaching the spacer-filled ch.
- ***α* affects significantly the mass transport**
- High polarization regions with *α0* → lower θ
- The shape of profiles is more influent for *α0*, where the circular shape allows higher θ
- In **diluted solutions θ** would be **much lower**

Influence of profiles' size *l* and pitch *L*

(c-α45, Re =8)

CONCENTRATION FIELD

Plane *x-z* middle

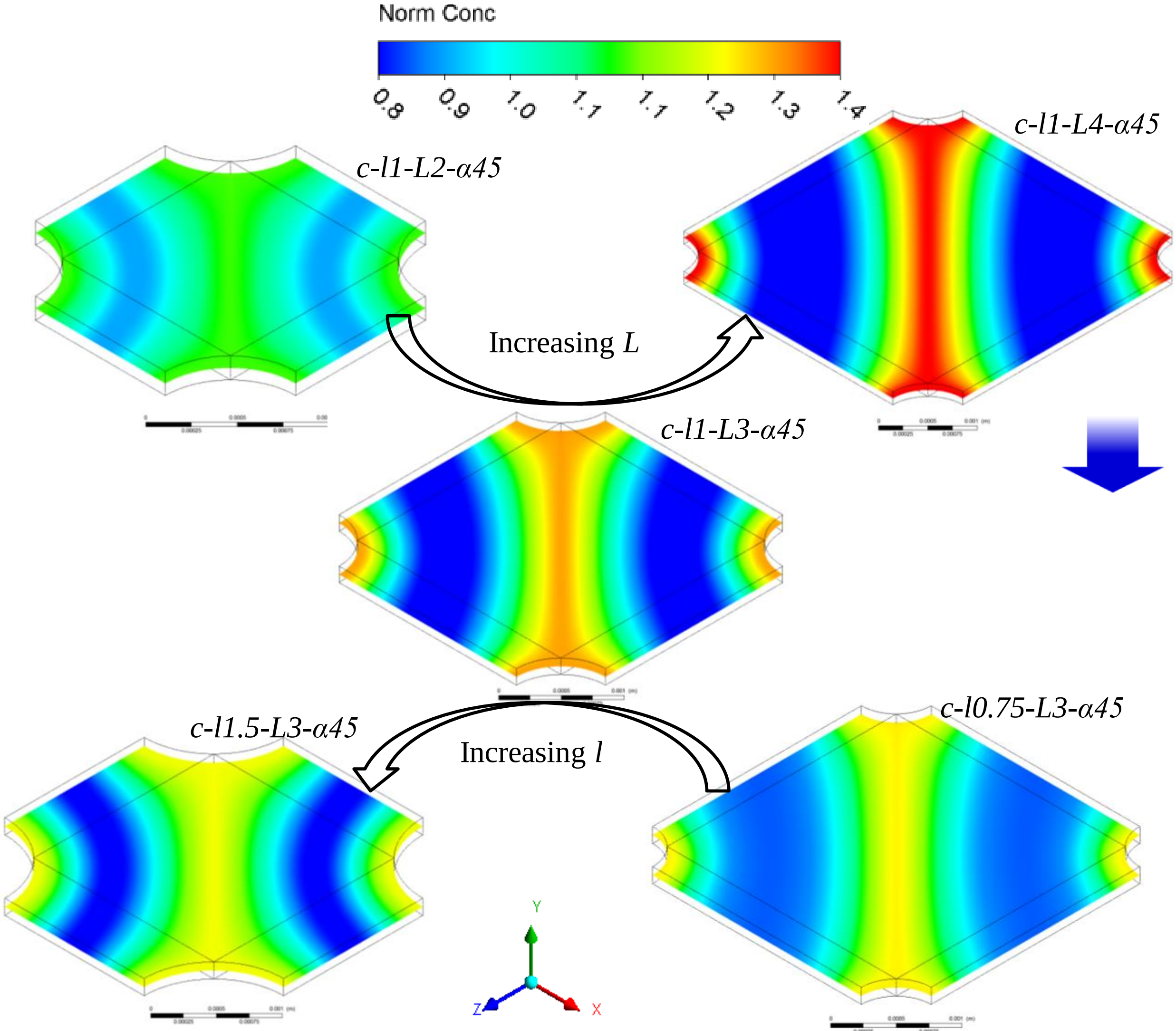

- Less uniform concentration field, as ***L*** increases
- Conversely, smaller variation as ***l*** decreases
- The highest polarization appears to be at the intermediate *l*
- **Different dependence of the mixing degree on the two parameters**

POWER NUMBER

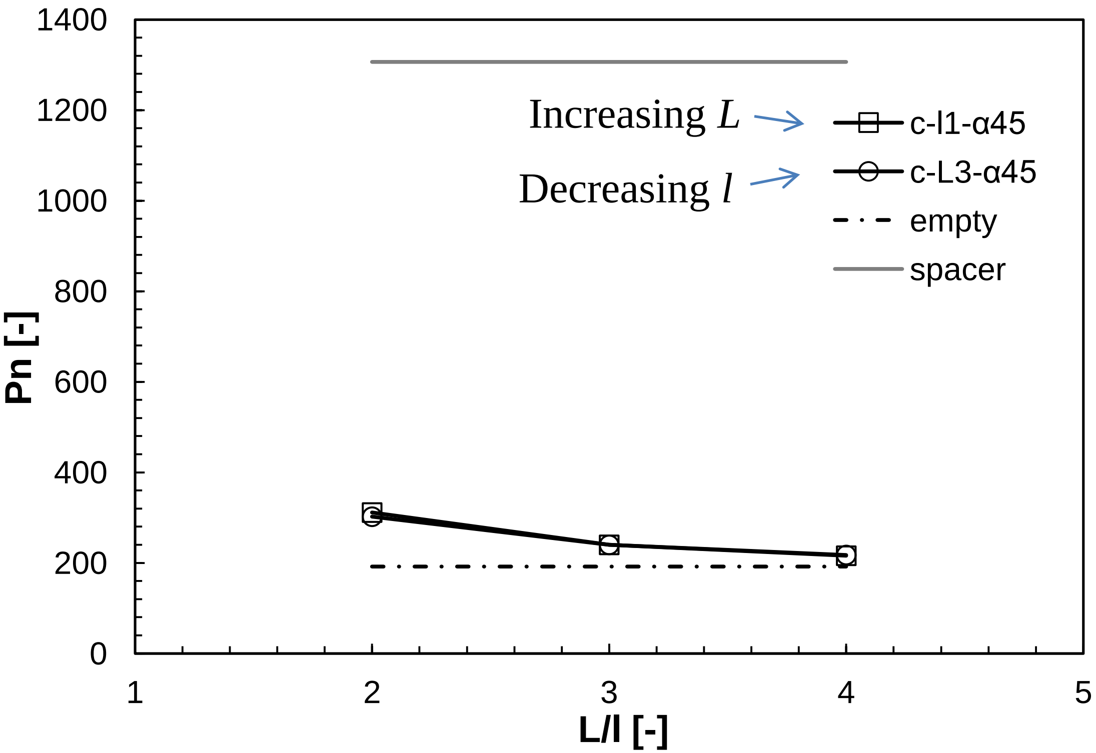

$$Pn = \mathrm{SPC}\frac{\rho^2 h^4}{\mu^3} = \frac{1}{8} f\, Re^3$$

$$\mathrm{SPC} = \frac{\Delta p}{l} u_{s,mean}$$

- As *L/l* increases, *f* is reduced and it will tend to attain the value relevant to the empty channel
- For a given ***L/l***, the absolute value of the **two parameters** has a **negligible impact**
- When *L/l* decreases → considerable increment of Pn, **up to 62% more than the empty ch.**
- Pn remains **noticeably lower than** the one exhibited by the **spacer-filled ch.**

POLARIZATION FACTOR

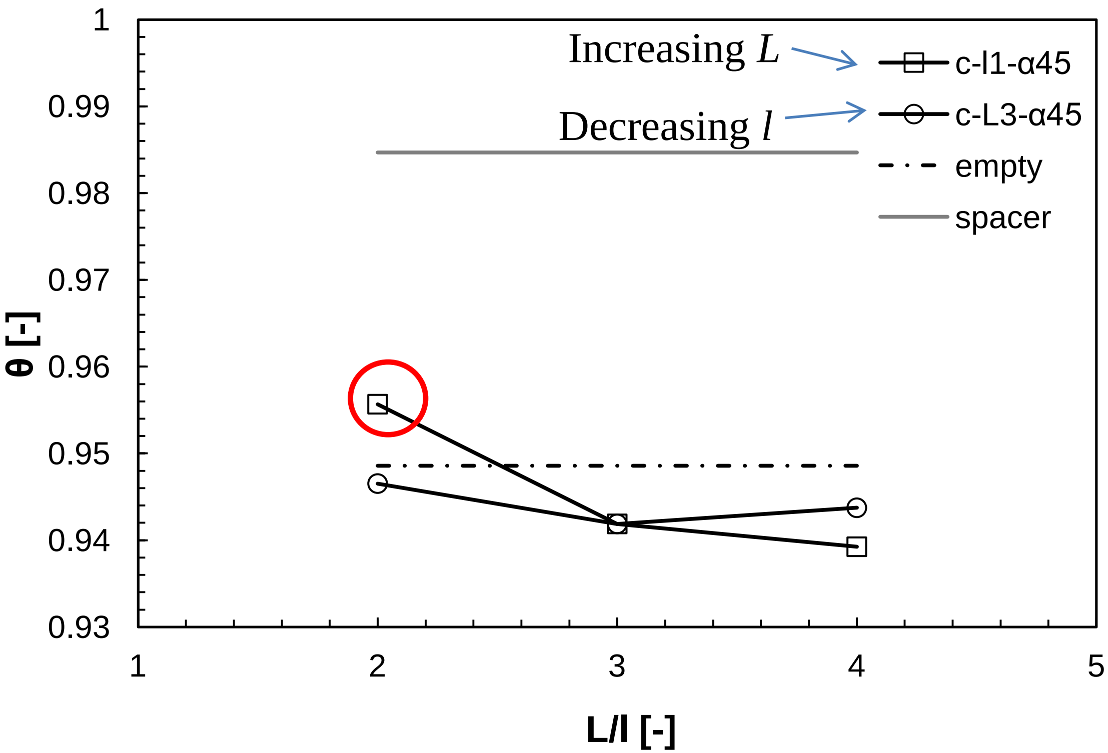

$$\theta = \frac{C_b}{C_i} < 1$$

- Increasing *L*, lower θ are obtained; conversely, as *l* decreases, the trend is not monotone (minimum value for the middle case)
- Maximum θ for *c-l1-L2-α45* which is also the case with the highest *f* and Pn
- Comparable θ is found respect to the empty ch.
- Mixing quite less favoured with respect to the spacer-filled ch.
- **Mass transfer enhancement achieved by filling more the channel, accomplished along with greater Pn→ performance similar to the spacer**

CONCLUSIONS

CONCLUSIONS

CFD modelling of Profiled Membranes ch. for RED

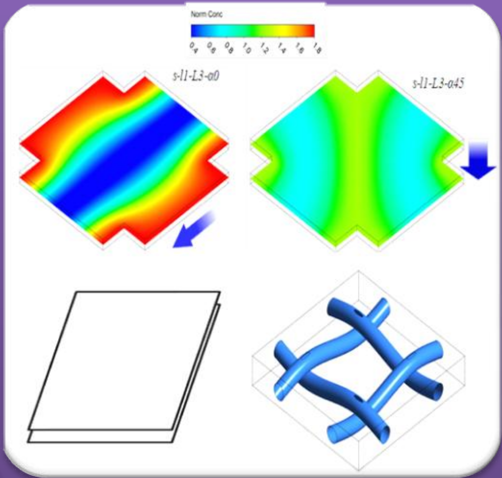

- Fluid flow and mass transfer behaviour
- Parametric analysis of:
    - Channel geometry
    - Channel orientation
    - Re effects
- Comparison with empty and spacer-filled channel
- Process efficiency: Pn and θ

OPTIMAL CHANNEL CONFIGURATION

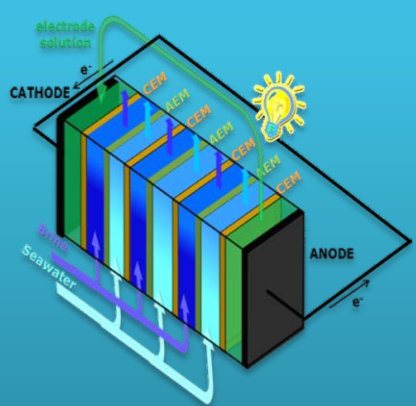

Influence of various factors on efficiency. Fundamental features of PM: significant reduction of pumping costs respect to a spacer and endless geometric possibilities. Suitable PM geometry and Re → better mixing, which, combined with the other advantages, could make the PM ch. the best choice for the optimization

Thank you for your attention

Luigi Gurreri

luigi-gurreri@unipa.it

EuroMed 2015

Desalination for Clean Water and Energy

Palermo, Italy, 10-14 May 2015

UNIVERSITÀ DEGLI STUDI DI PALERMO